



“Gheorghe Asachi” Technical University of Iasi, Romania



ELECTROCHEMICAL DEGRADATION OF CLINDAMYCIN BY ANODIC OXIDATION ON SnO₂-Sb COATED TITANIUM ANODES

Mitra Gholami^{1,2}, Mojtaba Davoudi^{2,3*}, Mehdi Farzadkia²,
Ali Esrafil², Abolghasem Dolati⁴

¹Research Center for Environmental Health Technology, Iran University of Medical Sciences, Tehran, Iran

²Department of Environmental Health Engineering, School of Public Health, Iran University of Medical Sciences, Tehran, Iran

³Health Sciences Research Center, Torbat Heydariyeh University of Medical Sciences, Torbat Heydariyeh, Iran

⁴Department of Materials Science and Engineering, Sharif University of Technology, Tehran, Iran

Abstract

Degradation of Clindamycin phosphate (CMP) was studied in aqueous solutions by an anodic oxidation process under galvanostatic conditions. The electrolysis cell consisted of a Ti/SnO₂-Sb anode, prepared by dip-coating technique, and a 316 stainless steel cathode, both of which had a surface area of 6 cm². The effects of critical factors, including CMP concentration, current density, initial pH, and the supporting electrolyte were evaluated. The electrochemical oxidation of CMP was controlled by mass transport within the studied range. The kinetic analysis indicated that the degradation reactions followed pseudo-first-order equation. The rate of CMP decay, as well as that of COD removal, decreased with increasing initial concentrations. Better Instantaneous Current Efficiency (ICE) values were obtained at higher organic concentrations, due mainly to the increased mass transfer flux towards non-active anode surface. Increasing current density and initial pH led to the faster removal of CMP, primarily because of enhanced electrogenerated hydroxyl radicals ([•]OH) on the anode surface. However, COD reduction was found to be pH independent. The removal rates of CMP and COD were also discussed with respect to the supporting electrolyte in different types and concentrations. The GC-MS analysis indicated that tert-butyl compounds were the major organic intermediates for the electrochemical degradation of Clindamycin.

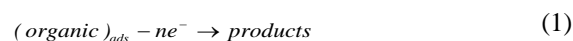
Keywords: clindamycin, electrochemical oxidation, hydroxyl radical, pharmaceutical compounds, SnO₂-Sb anodes

Received: July, 2013; Revised final: June, 2014; Accepted: June, 2014; Published in final edited form: February 2018

1. Introduction

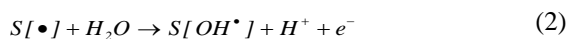
Advanced oxidation processes (AOPs) have been widely used to remove refractory organic pollutants from aqueous environments (Asgari et al., 2012; Grčić et al., 2017; Lutić et al., 2017). However, in recent years, a significant attention has been paid to the electrochemical oxidation technique as an alternative for AOPs because of its inherited characteristics such as ease of application, no need for chemicals usage and storage, close control of desirable reactions simply by adjusting current intensity, and so on (Bagastyo et al., 2012). In this process, partial or

complete oxidation of organics can be achieved by direct and/or indirect mechanisms. In the direct oxidation, molecules of the pollutant are first adsorbed on the anode surface and then oxidized by direct electron transfer, as presented in Eq. (1) (Li et al., 2005):

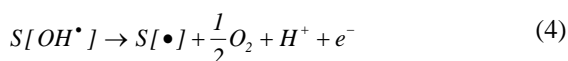


In indirect oxidation, oxidizing mediators such as [•]OH radicals resulted from anodic water discharge, react with organics to oxidize them on the anode surface, expressed as Eqs. (2) and (3) (Panizza and Cerisola, 2005):

* Author to whom all correspondence should be addressed: e-mail: Davoudi85@gmail.com; Phone: +9821 88779118; Fax: +9821 88779487



where: $S[\bullet]$ represents the anodic sites for the adsorption of $\bullet OH$ species, and R represents the molecules of the organic pollutant. Alternatively, $\bullet OH$ radicals can be discharged to dioxygen molecule, which is considered an undesirable side reaction for electrochemical mineralization (Eq. 4) (Panizza and Cerisola, 2005):



The anode material has a great influence on taking place the organic combustion reaction in Eq. (3) or the oxygen evolution reaction in Eq. (4). The active electrodes strongly react with $\bullet OH$ radicals and favor the dioxygen-evolution reaction. Platinum (Asazawa et al., 2009; Li et al., 2009; Tavares et al., 2012; Zhao et al., 2008), carbon (Abdel-Hamid et al., 2016; Belhadj Tahar and Savall, 2009), graphite (Chen et al., 2010; Goyal et al., 2008; Kong et al., 2011), and some metal oxide anodes, such as IrO_2 (Chatzisyseon et al., 2009; Zaviska et al., 2011), RuO_2 (Jeong and Lee, 2012), and IrO_2/RuO_2 (Radjenovic et al., 2011; Raghu et al., 2009; Turro et al., 2011) are all of active materials. On the other hand, the non-active anodes such as Boron-doped diamond (BDD), lead dioxide (PbO_2), and tin dioxide (SnO_2) exhibit a poor affinity for $\bullet OH$ radicals and favor organics mineralization (Martínez-Huitle et al., 2008; Sirés and Brillias, 2012). Hence, non-active materials are believed to be the most appropriate anodes for water and wastewater treatment purposes. In spite of some advantages, high preparation cost and possible release of poisonous Pb^{2+} are the main disadvantages associated with BDD and PbO_2 anodes, respectively, making their commercial production and utilization less attractive (Panizza and Cerisola, 2005; Song et al., 2010; Wang et al., 2006).

Contrary, simple preparation techniques and cleaner materials in the layer are the main advantages of SnO_2 anodes (Chen et al., 2009; Wang et al., 2006). Small amounts of antimony (Sb) are usually doped to SnO_2 film to enhance its electrical conductivity (Feng and Li, 2003). Over the past few years, effectiveness of SnO_2 -Sb thin film has been proved for partial and/or complete oxidation of biologically refractory organic pollutants such as phenol and its derivatives (Chen et al., 2005; Davoudi et al., 2014; Feng and Li, 2003; Song et al., 2010), herbicide atrazine (Zaviska et al., 2011), β -blocker metoprolol (Radjenovic et al., 2011), and C.I. Reactive Orange 4 (Del Rio et al., 2009). However, the major drawback of SnO_2 anode is its service life, which has been reported a few hours or even much less in some studies (Montilla et al., 2004). Nevertheless, it has been proven that the stability of SnO_2 film can be enhanced by adding new dopants, including Ni (Wang et al., 2006), Ce (Chen et al.,

2009), Pt, Ir (Costa et al., 2010; Vicent et al., 1998), Ru (Chen and Chen, 2005), and Ce-Ru (Liu et al., 2012)

In the recent years, there have been growing concerns over Pharmaceutically Active Compounds (PhACs), such as antibiotics, in wastewater effluents, surface water, and groundwater (Martinez, 2009). Clindamycin is a chlorinated lincosamide antibiotic that has a wide clinical application against gram-positive bacteria (Ravikumar and Sridhar, 2010; Verdier et al., 2000). A literature survey showed that its removal from aqueous solutions has been tried by techniques such as photocatalytic degradation using nano-ZnO catalysts (Farzadkia et al., 2014) and oxidative degradation using nanoscale zero-valent iron/ H_2O_2 /US (Gholami et al., 2016). The main objective of the present study was to evaluate the ability of Ti/ SnO_2 -Sb electrode for anodic oxidation of clindamycin phosphate (CMP) in a synthetic wastewater.

2. Experimental

2.1. Chemicals

The antibiotic Clindamycin phosphate (CMP) ($C_{18}H_{34}ClN_2O_8PS$), purchased from Sigma-Aldrich, was of analytical grade and used without further purification. CMP stock solution was prepared with double-distilled water (DDW) with a resistivity of $18.2 \text{ M}\Omega \text{ cm}$ at 25°C . All other chemicals were also of analytical grade. Electrolytic solutions were prepared by using Na_2SO_4 , $NaNO_3$, and $NaCl$, all supplied by Merck. The initial pH of the electrolyte solutions was adjusted using H_2SO_4 and $NaOH$. Chemicals used for anode preparation were $SnCl_4 \cdot 5H_2O$ (purity, 97.5%, BDH), $SbCl_3$ (purity, 99%, CDH), isopropanol (purity, 99.8%, Merck), and hydrochloric acid (purity, 37%, Merck).

2.2. Preparation of Ti/ SnO_2 -Sb electrode

Titanium plates (grade 2, $20 \text{ mm} \times 15 \text{ mm} \times 1 \text{ mm}$) were used as the substrate after being treated by the method described in the literature (He et al., 2011; Song et al., 2010). Thin films of SnO_2 -Sb were grown on the pretreated substrates by a dip-coating technique described by Chen et al. (2005). The precursor solution contained a molar ratio of Sb:Sn=6:94 in 2.5 mL of concentrated HCl and 50 mL of isopropanol as the solvent. The prepared electrodes were measured to have a total oxide loading of 6.5 mg cm^{-2} .

2.3. Electrolysis

Electrochemical degradation of CMP was conducted on a single compartment cell consisted of a Ti/ SnO_2 -Sb electrode as the anode and a 316-stainless steel with the same dimensions as a cathode. The distance between the anode and cathode plates was kept at 10 mm. Solutions were prepared by diluting a required amount of CMP stock solution with DDW.

After adding the supporting electrolyte and adjusting pH, prepared solutions of 450 mL were electrochemically treated at room temperature using a DC power supply under galvanostatic conditions. A magnetic stirrer was used for providing continuous mixing and enhancing the mass transfer. Samples were collected at preset intervals for chemical analysis of CMP, as well as to determine the chemical oxygen demand (COD) and organic intermediate products.

2.4. Analysis

Before chemical analysis, samples were filtered through 0.45 μm PTFE Whatman filters. The concentration of CMP during electrochemical degradation process was determined by a high-performance liquid chromatography (CECIL CE 4100 HPLC) instrument equipped with a C18 column (5 μm; 250 mm × 4.6 mm; MZ-Analysentechnik) and a UV-Visible Diode Array detector, which was operating at the working wavelength of 274 nm. The mobile phase was an 80:20 (v/v) methanol/buffer mixture at a flow rate of 1 mL min⁻¹. The buffer solution consisted of 10 mM hexane sulfonic acid and 20 mM citric acid, adjusted at pH 3.4 with NaOH. The injection volume of aliquots was 20 μL. A well-defined peak was observed at a retention time of 3.35 min.

The organic concentration in the solution was measured by the COD method based on the Standard Methods for the Examination of Water and Wastewater (Eaton et al., 2005). The COD values were used for evaluating the kinetics of organic matter decay as well as for calculating the instantaneous current efficiency (ICE) using Eq. (5) (Gao et al., 2009):

$$ICE = [(COD_t - COD_{t+\Delta t})/8I\Delta t]FV \quad (5)$$

In the previous equation, COD_t and $COD_{t+\Delta t}$ are the chemical oxygen demand (in g O₂ L⁻¹) at times t and $t + \Delta t$ (s), respectively, F is the Faraday constant (96487 C mol⁻¹), V is the volume of the electrolyte (L), I is the current (A), and 8 is the equivalent mass of oxygen (g eq⁻¹).

The energy consumption was calculated and expressed in terms of kWh per unit volume of the electrolyzed solution and kWh per unit mass of the removed COD, according to Eqs. (6) and (7), respectively (Guinea et al., 2010; Najafpoor et al., 2017; Zhu et al., 2010;):

$$EC = U_{cell}It/V \quad (6)$$

$$EC = U_{cell}It/[(COD_{in} - COD_{out})V] \quad (7)$$

In the above equations, EC is the energy consumption (kWh m⁻³ or kWh kgCOD⁻¹), U_{cell} is the average cell potential (V), t is the electrolysis time (h), and COD_{in} and COD_{out} are the influent and effluent COD of solution (g O₂ L⁻¹). The anode efficiency (AE)

was calculated according to Eq. (8) (Arapoglou et al., 2003):

$$AE = [(COD_{in} - COD_{out})V]/ItA \quad (8)$$

where: AE is the anode efficiency (gCOD h⁻¹ A⁻¹ m⁻²), t is the electrolysis time (h), and A is the surface area of the anode (m²).

In order to detect organic by-products of CMP degradation, a liquid-liquid solvent extraction was performed by adding 5 mL of hexane (HPLC grade, Merck) to the electrolyzed sample. A gas chromatography instrument coupled with a mass spectrometer (GC-MS) was used to detect organic intermediates. The GC instrument comprised an Agilent (Centerville Road, Wilmington, USA) series 7890A GC coupled with an Agilent MSD 5975C quadrupole mass spectrometer. The GC instrument had an HP-5 MS capillary column (30 m × 0.32 mm i.d., 0.25 μm film thickness) from Agilent J&W Scientific (Folsom, CA, USA). Helium (99.999%) was used as the carrier gas at 1.0 mL min⁻¹. The following temperature program was employed: 50 °C for 1 min, increased temperature to 280 °C at 10 °C min⁻¹ and held for 5 min. The MS quadrupole and the MS source temperatures were set at 150 °C and 250 °C, respectively. The electron impact (EI) mass spectra were obtained at an acceleration energy of 70 eV. In addition, 1 μL aliquot of the extract was auto injected by Agilent series 7683 automatic liquid sampler (Centerville Road, Wilmington, USA) in the splitless mode.

3. Results and discussions

A set of experiments were carried out under galvanostatic conditions to investigate the effect of a variety of parameters, such as initial concentration of the contaminant, current density, initial pH of the solution, and supporting electrolyte, on the electrochemical abatement of clindamycin phosphate (CMP).

3.1. Effect of initial concentration

450 mL working solutions containing CMP concentrations of 100, 200, and 400 mg L⁻¹ (corresponding to 128, 264, and 458 mg L⁻¹ of COD) and 0.10 M Na₂SO₄ were initially electrolyzed at pH 7 and a constant applied current density (j_{app}) of 33.33 mA cm⁻². Fig. 1 depicts the trend of CMP decay as a function of electrolysis period at three different initial concentrations. As can be seen, the rate of degradation was much faster at the initial concentration of 100 mg L⁻¹. Additionally, there was no much difference in the degradation rate of CMP when the concentration increased from 200 to 400 mg L⁻¹.

For example, at the electrolysis time of 180 min, the extent of degradation was 90% for the initial concentration of 100 mg L⁻¹, whereas at the same period, about 70% of CMP was degraded at initial concentrations of 200 and 400 mg L⁻¹.

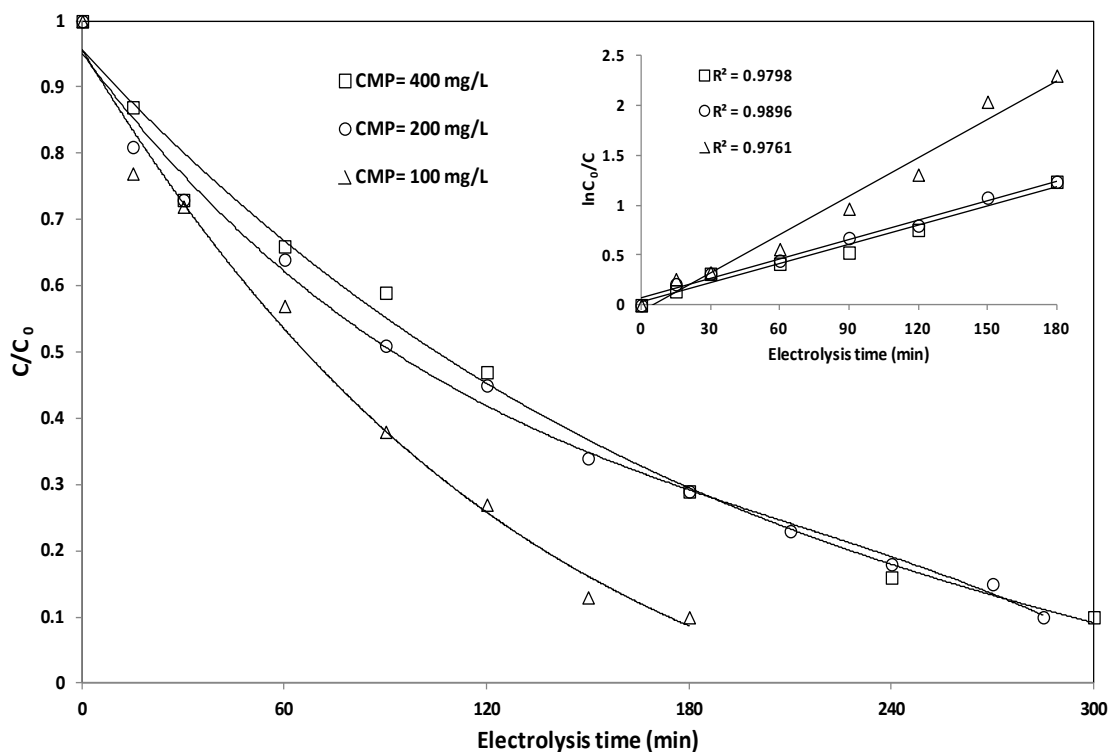


Fig. 1. Decay of different initial concentrations of CMP at 33.33 mA cm⁻² (electrolyte, 0.10 M Na₂SO₄; pH, 7). Inset: corresponding kinetic analysis assuming pseudo-first order reaction for CMP decay

The kinetic study revealed that the degradation of CMP best fitted to the pseudo-first-order equation, as earlier studies indicated for the most of organic compounds (Dalvand et al., 2011; Hmani et al., 2009; Li et al., 2010; Samet et al., 2006; Sirés et al., 2008). The inset of Fig. 1 indicates the straight lines for three levels of the initial concentration during 180 min of electrolysis time. The pseudo-first-order rate constants (k values) were 0.21×10^{-3} , 0.11×10^{-3} , and $0.10 \times 10^{-3} \text{ s}^{-1}$ for 100, 200, and 400 mg L⁻¹, respectively.

Decreasing degradation rates with an increase in the initial concentration have also been reported by Boye et al. (2006), Muruganathan et al. (2007), and Najafpoor et al. (2017). This can be explained by assuming that at a fixed applied current density, a constant rate of $\cdot\text{OH}$ radical was electrogenerated from water discharge at the SnO₂-Sb anode surface. When the ratio of $\cdot\text{OH}$ to CMP molecules was high, the mediated oxidant attacked the lower concentration of the pollutant and destruction occurred at a short period. In contrast, when the ratio was low, occurring at higher organic concentrations, degradation of CMP initiated through reaction with $\cdot\text{OH}$ and high-weight organic intermediates were formed. As a result, part of $\cdot\text{OH}$ radicals was consumed for degradation of newly generated compounds; and hence, fewer amounts remained for CMP destruction.

The effect of initial CMP concentration was also examined on the performance of the electrooxidation process for COD removal, and the results obtained are illustrated in Fig. 2. As shown, complete oxidation was not achieved under the

experimental conditions even after 300 min electrolysis. However, the rate of COD removal was found to be higher at lower initial concentrations. The COD removals of 85%, 69%, and 64% were obtained at the end of the electrolysis time for the initial COD concentrations of 128, 264, and 458 mg L⁻¹, respectively. Based on the obtained results, the kinetic analysis of COD removal is presented in the inset of Fig. 2, which indicates that the oxidation reactions were in agreement with pseudo-first-order equation ($R^2 > 0.99$). In this case, the slope of the $\ln(\text{COD}_0/\text{COD}_t)$ plot versus the electrolysis time gives the apparent rate constant (k_{app}) of COD removal (Samet et al., 2010). The k_{app} value is used to calculate the average mass transfer coefficient (k_m) towards the electrode surface from Eq. (9):

$$k_{app} = Ak_m/V \quad (9)$$

where A is the electrode area (m²) and V is the volume of the treated solution (m³).

The k_{app} values were 10.2×10^{-5} , 6.3×10^{-5} , and $5.7 \times 10^{-5} \text{ s}^{-1}$ for initial COD concentrations of 128, 264, and 458 mg L⁻¹, respectively, which give k_m values of 7.65×10^{-5} , 4.72×10^{-5} , and $4.27 \times 10^{-5} \text{ m s}^{-1}$. These findings are in agreement with those previously reported in the literature (Boye et al., 2006; Samet et al., 2010) and can be attributed to the formation of major intermediate compounds that were hardly decomposed into CO₂ and water when a higher concentration of organics was introduced into the electrolysis cell. However, the removed quantity of

COD (in mg L⁻¹) increased as the initial concentration increased. For example, at electrolysis time of 120 min, the COD removal values were 60, 90, and 174 mg L⁻¹ for initial concentrations of 128, 264, and 458 mg L⁻¹, respectively. Samet et al. (2010) defined the overall mass transfer rate as a parameter expressed as $k_m \cdot COD_t$. Considering COD concentrations at the time of zero, these values were 9.79×10^{-3} , 12.46×10^{-3} , and

$19.56 \times 10^{-3} \text{ g m}^{-2} \text{ s}^{-1}$ for initial COD concentrations of 128, 264, and 458 mg L⁻¹, respectively. This tendency confirmed more diffusion of organic mass to the anode surface at high initial concentrations. The observation is better reflected in Fig. 3, which depicts the obtained data for Instantaneous Current Efficiency (ICE) as a function of specific electrical charge (Q) and initial COD concentration.

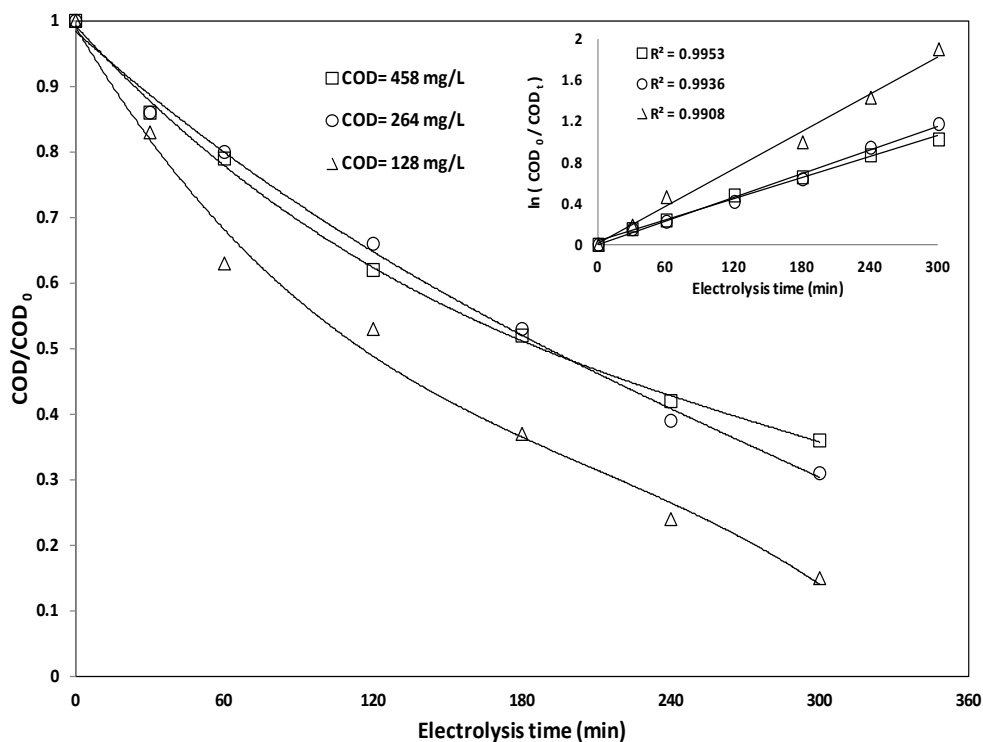


Fig. 2. COD removal for three different initial COD at 33.33 mA cm⁻² (electrolyte, 0.10 M Na₂SO₄; pH, 7). Inset: corresponding linear regression for COD removal with electrolysis time

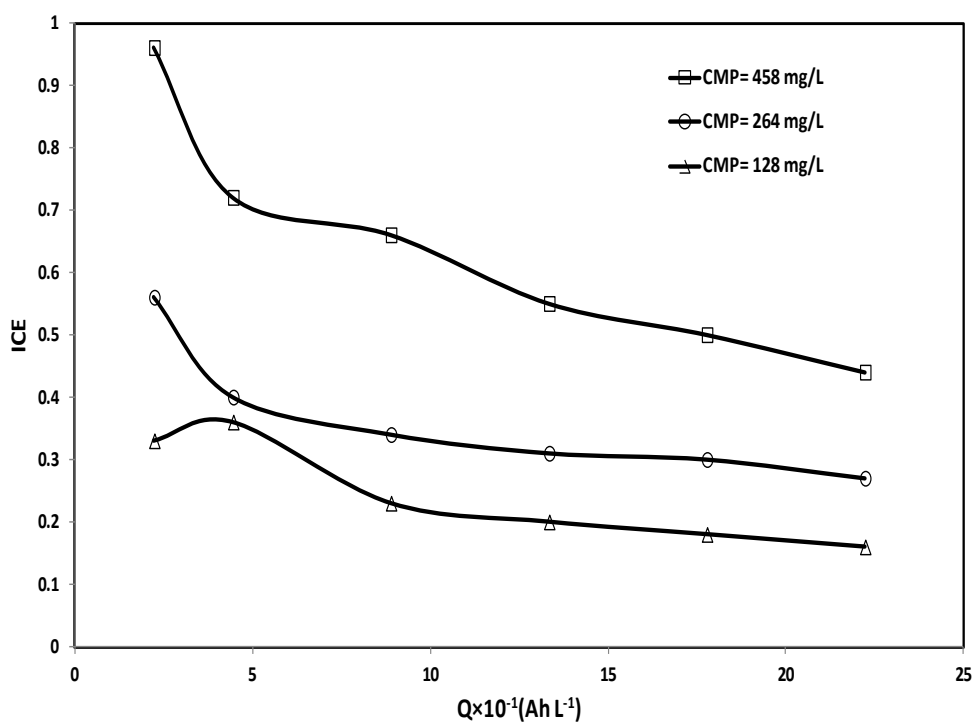


Fig. 3. Instantaneous current efficiency versus specific electrical charge for the COD removal results shown in Fig. 2

Maximum efficiencies during the entire electrolysis time belonged to an initial concentration of 458 mg L⁻¹. This behavior indicates that fewer amounts of •OH radicals were wasted in parallel reactions such as dioxygen formation when the organic content of the solution was higher (Muruganathan et al., 2008; Samet et al., 2006). It is also noteworthy that a similar trend for ICE values was shown for initial concentrations of 264 and 458 mg L⁻¹. In this case, the ICE curve indicated a sharp decrease down to a Q-value of 0.444 A h L⁻¹ during the initial phase of the electrolysis time, whereas the obtained curve for the concentration of 128 mg L⁻¹ slightly increased during the same period of time. The latter could be explained by the fragmentation of CMP into lower molecular weight intermediates that were subjected to the rapid oxidation at initial stages of the electrolysis process. However, except for the beginning phases, a similar trend for ICE values was observed in all three of the initial concentrations. The decreasing trends for ICE values with increasing electrolysis period have also been reported in earlier studies and could be attributed to the formation of intermediates with higher stabilities than those of easily oxidizable compounds produced during the initial stages of the electrolysis process (Muruganathan et al., 2008; Samet et al., 2010).

It has been well established that anodic oxidation processes in electrolysis cell are controlled by either applied current density or mass transfer rate. In order to determine the working regime of an electrolysis cell, we calculated the limiting current density (j_{lim}) by using Eq. (10), described by Panizza and Cerisola (2005):

$$j_{lim}(t) = 4Fk_m COD(t) \quad (10)$$

where: $j_{lim}(t)$ is the limiting current density (A m⁻²) at a given time t (s), k_m is the mass transfer coefficient (m s⁻¹), and COD is the chemical oxygen demand (mol O₂ m⁻³). In an electrolysis cell, if j_{appl} is lower than j_{lim} , oxidation reactions are limited by current density and current efficiency is 100% (Panizza et al., 2001).

In the present study, maximum values for j_{lim} at the beginning of the electrolysis process were 11.81, 15.03, and 23.59 mA cm⁻² at initial COD concentrations of 128, 264, and 458 mg L⁻¹, respectively. Considering an applied current density of 33.33 mA cm⁻², it can be concluded that the electro-oxidation process on the Ti/SnO₂-Sb anode was controlled by organic matter diffusion flux. This is consistent with all calculated ICE values that were below the unity.

3.2. Effect of current density

The electrochemical degradation of CMP was studied at an initial concentration of 200 mg L⁻¹ at the presence of 0.1 M Na₂SO₄ as the supporting electrolyte at pH 7 by applying current densities of 16.66, 33.33, and 66.66 mA cm⁻². Fig. 4 illustrates the concentration-time profile for CMP decay at different j_{appl} . It can be seen that anodic oxidation was capable of nearly complete CMP destruction, regardless of the applied current density.

However, the rate of decomposition proportionally increased with an increase in j_{appl} . For example, 90% removal was achieved after 320, 285, and 210 min of the electrolysis at applied current densities of 16.66, 33.33, and 66.66 mA cm⁻², respectively. It should be noted that under experimental conditions, the degradation reaction was limited mainly by diffusion.

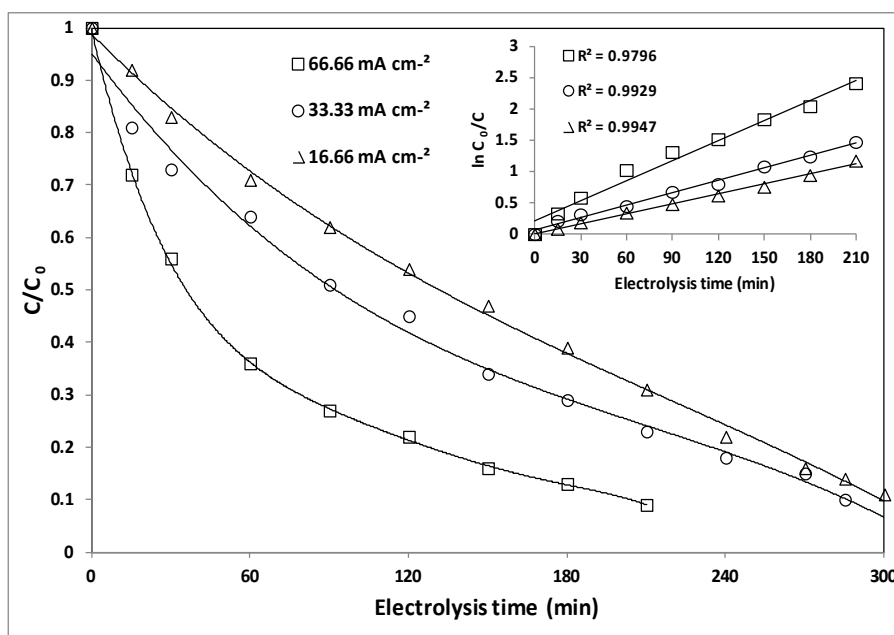


Fig. 4. Effect of applied current density on CMP degradation (CMP concentration, 200 mg L⁻¹; electrolyte, 0.10 M Na₂SO₄; pH 7). Inset: corresponding kinetic analysis assuming pseudo-first order reaction for CMP decay

Under such circumstances, oxygen evolution reaction was favored and large amounts of O₂ released to the reaction solution, according to Eq. 4. Gas bubbles enhanced the mass transfer rate of the organic molecules towards the anode surface to react with physically adsorbed hydroxyl radicals (Belhadj Tahar et al., 2009; Samet et al., 2006). Boye et al. (2006) and Song et al. (2010) also reported that increasing j_{app} increases degradation rates, which can be attributed to the formation of more $\cdot\text{OH}$ at the anode surface at higher current densities. Higher applied current densities also intensified the production of mediated oxidants such as peroxodisulphate (S₂O₈²⁻) generated during the oxidation of SO₄²⁻, hydrogen peroxide (H₂O₂), and ozone (O₃) from water discharge, according to Eqs. (11) to (13) (Michaud et al., 2003):

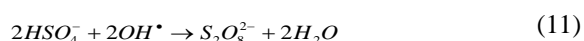


Fig. 4 also reveals that at the end of the electrolysis process, the extent of degradation was irrespective of the applied current densities of 16.66 and 33.33 mA cm⁻² since the CMP removal efficiencies were very close to each other from 240 to 300 min electrolysis. This could be attributed to the fact that as electrolysis proceeded, less mass of the pollutant remained in the solution to transfer to the electrode surface (Samet et al., 2010).

The kinetic study demonstrated that CMP degradation followed a pseudo-first-order reaction. The inset of Fig. 4 shows the straight lines for three levels of current density at 210 min of the electrolysis time. The corresponding k values were 0.88×10^{-4} , 1.1×10^{-4} , and $1.78 \times 10^{-4} \text{ s}^{-1}$ for 16.66, 33.33, and 66.66 mA cm⁻², respectively. The k values increased with the applied current densities of 33.33 and 66.66 mA cm⁻², indicating that the degradation process occurred primarily due to the reaction of CMP with electrogenerated mediated oxidants such as hydroxyl radicals (Muruganathan et al., 2008).

3.3. Effect of initial pH

The influence of initial pH values (4, 7, and 10) was studied at a constant applied current density of 33.33 mA cm⁻² in solutions containing 200 mg L⁻¹ CMP in the presence of 0.10 M Na₂SO₄ as the supporting media. The pH of the solutions slightly increased with electrolysis time.

This behavior was also reported by Muruganathan et al. (2010) and Rajkumar et al. (2005) and could be due to the consumption of hydrogen ions in the cathodic reaction shown in Eq. (14):



It is observed in Fig. 5 that the degradation of CMP occurred more efficiently under alkaline conditions, compared to neutral or acidic conditions.

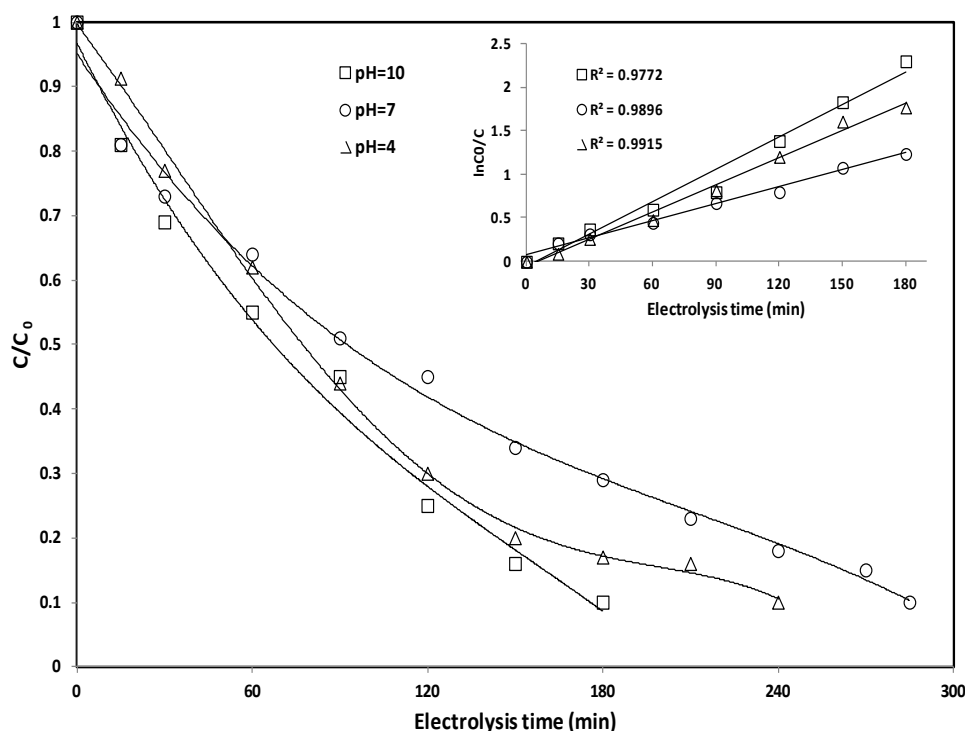


Fig. 5. Dependence of CMP degradation with respect to initial pH of the electrolyte (CMP concentration, 200 mg L⁻¹; current density, 33.33 mA cm⁻²; electrolyte, 0.10 M Na₂SO₄). Inset: corresponding kinetic analysis assuming pseudo-first order reaction for CMP degradation

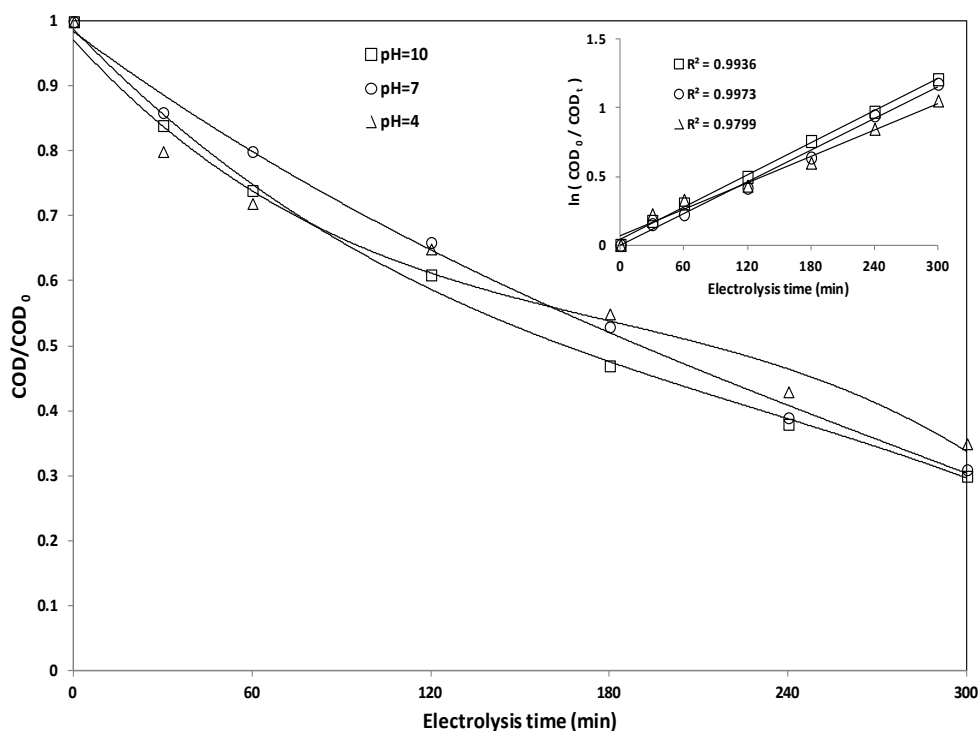


Fig. 6. Influence of the initial solution pH on COD removal during electrochemical oxidation of CMP (CMP concentration, 200 mg L⁻¹; current density, 33.33 mA cm⁻²; electrolyte, 0.10 M Na₂SO₄). Inset: corresponding linear regression for COD removal with electrolysis time

The degradation of 90% was obtained after 180 min of the electrolysis time at an initial pH of 10, while the same efficiency was achieved after electrolysis period of 285 and 240 min at initial pHs of 7 and 4, respectively. The corresponding rates of degradation were found to be 2.07×10^{-4} , 1.08×10^{-4} , and 1.73×10^{-4} s⁻¹. A similar outcome was also reported by Muruganathan et al. (2008) for anodic oxidation of bisphenol A. This can be due mainly to the fact that the formation of $\cdot\text{OH}$ radical was intensified by increasing OH⁻ concentrations in the solution by Eq. (15), as described by Brillas et al. (2005):



The CMP behavior as a function of pH is also worthy of mention. Clindamycin phosphate has two acidic protons with $\text{pK}_1=0.964$ and $\text{pK}_2=6.06$, meaning that this compound is completely ionized in alkaline solutions (Kipp et al., 1991). Therefore, CMP appeared as the anionic form at pH 10 and was attacked more strongly by electrophilic $\cdot\text{OH}$ radicals. Muruganathan et al. (2008) have also suggested this mechanism for anodic oxidation of bisphenol A at BDD electrode. The better performance of anodic oxidation at an initial pH 4 than that of pH 7 could be related to the enhanced oxidative potential of $\cdot\text{OH}$ and $\text{S}_2\text{O}_8^{2-}$ under acidic conditions (Polcaro et al., 2005; Serrano et al., 2002).

Fig. 6 indicates the effect of electrolysis time and initial pH on COD removal. Complete oxidation of CMP at initial pH values of 10, 7, and 4 was approximately 70%, 69%, and 65%, with k_m values of

4.87×10^{-5} , 4.75×10^{-5} , and 4.0×10^{-5} m s⁻¹, respectively. These data suggest that by-products of CMP degradation seemed to behave irrespectively of solution pH, and their oxidation rates were nearly equal at all three pH levels. Palma-Goyes et al. (2010) also could not make an overall indicator for the mineralization of crystal violet as a function of initial pH.

3.4. Effect of supporting electrolyte

Solutions containing 200 mg L⁻¹ CMP adjusted at pH 7 were electrochemically treated in the presence of Na₂SO₄, NaNO₃, and NaCl supporting electrolytes, all of which at concentrations of 0.05, 0.10, and 0.20 M. The results obtained at an applied current density of 33.33 mA cm⁻² are presented in Table 1. In the electrochemical oxidation process, supporting electrolytes are primarily added to enhance the electron transfer rate in the solution. In addition, some electrolytes are decomposed and turned into intermediate oxidants participating in the organic oxidation reaction (Zhang et al., 2012).

It has been proven that electrolyte decomposition is intensified at the mass transfer control regime because of higher applied current densities (Samet et al., 2010). Under such conditions, the oxidation process occurs not only at the anode surface by hydroxyl radicals but also at the bulk solution by inorganic oxidizing species (Bensalah et al., 2009; Panizza and Cerisola, 2005). Based on the data presented in Table 1, CMP removal was higher at SO₄²⁻ electrolyte compared to the NO₃⁻ solution.

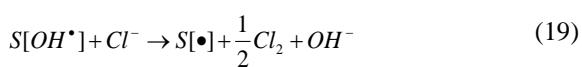
Table 1. Extent of CMP and COD removal along with electrolysis parameters as a function of supporting electrolyte during electrochemical oxidation of 200 mg L⁻¹ CMP at pH 7 and 33.33 mA cm⁻²

Electrolysis condition		CMP Degradation (%)			COD removal (%)			U _{cell} (V)	EC (kWh m ⁻³)	EC (kWh kgCOD ⁻¹)	AE (gCOD h ⁻¹ A ⁻¹ m ⁻²)
		1 h	3 h	5 h	1 h	3 h	5 h				
Na ₂ SO ₄	0.05M	26	65	88	13	39	62	8.5	18.9	115.4	122.76
	0.10M	37	71	93	20	47	69	7.4	16.5	90.3	136.62
	0.20M	35	68	95	26	51	70	6.5	14.4	78.1	138.60
NaNO ₃	0.05M	20	51	72	11	40	63	11.2	24.9	149.6	124.74
	0.10M	26	62	81	16	45	64	8.5	18.8	111.8	126.72
	0.20M	29	63	85	23	49	66	6.9	15.3	88.0	130.68
NaCl	0.05M	98.	–	–	27	38	48	11.3	25.1	198.2	95.04
	0.10M	99.	–	–	34	43	52	9	20.0	145.7	102.96
	0.20M	99.	–	–	34	47	59	6.6	14.6	94.3	116.82

This can be due to the fact that during the electrolysis with non-active anodes, sulfate ions can be converted to powerful oxidants such as sulfate radicals and/or peroxodisulfate ions (Bensalah et al., 2009; Muruganathan et al., 2010; Serrano et al., 2002) (Eqs. 16 to 18):



These active species combined with [•]OH radicals attacked the CMP molecules, leading to an increase in the degradation rate. On the contrary, nitrate ions make an inert electrolyte with no additional oxidants in the electrochemical oxidation process (Yoshihara and Muruganathan, 2009). Hence, in solutions containing NaNO₃, moderate degradation occurred solely by activation of [•]OH radicals. A similar outcome has been also obtained for the abatement of ketoprofen by using BDD electrodes (Muruganathan et al., 2010). However, the electrochemical cell did not show a significant difference in the oxidation rate of CMP when Na₂SO₄ or NaNO₃ electrolytes were used. It seems that the intermediates resulted from SO₄²⁻ decomposition were not powerful enough to degrade persistent organic by-products. Table 1 demonstrates that the trend of CMP removal in NaCl solution was very different. In this case, CMP was completely removed at an electrolysis time of 60 min. This can be due to *in situ* generation of strong oxidants such as HOCl and OCl⁻ (Ahmed Basha et al., 2010), according to Eqs. (19) to (22):



In the present study, these inorganic oxidizing agents combined with [•]OH radicals caused the faster removal of CMP, which is in agreement with the findings of previous works dealing with electrooxidation of other organic pollutants (Muruganathan et al., 2007, 2010). NaCl electrolyte, however, could not lead to the improved COD removal. This has also been previously reported in the literature (Muruganathan et al., 2008; Yoshihara and Muruganathan, 2009) and could be attributed to the formation of slowly degradable organochlorinated compounds. We found that at initial stages of the electrolysis time, the reaction solution attained a clear yellow color, which appeared more intense at higher NaCl concentrations. At NaCl concentration of 0.20 M, a weak foam was also formed at the surface of solution, which could be a sign of polymeric compounds formation that neither active chlorine species nor hydroxyl radicals were able to oxidize them (Brillas et al., 2005; Costa et al., 2009; Li et al., 2005; Skoumal et al., 2008). In addition, it was observed that the solution pH increased from neutral to slightly basic during the electrolysis process. The alkaline pH could lower the oxidative potential of [•]OH and other intermediate oxidants, as shown by Costa et al. (2009) for the electrochemical oxidation of acid black 210 at the presence of chloride ions.

Table 1 also presents the energy consumption as a function of the type and concentration of the supporting electrolyte after 5 h electrolysis. Under galvanostatic conditions, the energy consumption of electrolysis is related to the anode material, design of electrolysis cell, pH of the solution, and type and concentration of the supporting electrolyte (Bensalah et al., 2009; Costa et al., 2009; Guinea et al., 2010). In the present work, as expected, the estimated energy consumption per unit volume of the treated wastewater decreased with increasing electrolyte concentrations. This can be due to the low average cell voltage (*U*_{cell}) as a response to the increased conductivity of the solution. The minimum values were observed in the presence of Na₂SO₄ salt, because

sulfate is a divalent anion, making a stronger electrolyte compared to monovalent nitrate and chloride ions. Moreover, $S_2O_8^{2-}$ anions formed by decomposition of SO_4^{2-} further improved the ionic conductivity of wastewater (Zhang et al., 2012). It should be noted that in an electrochemical cell, especially in diffusion control, part of the applied energy is lost via increasing the solution temperature and developing unwanted side reactions such as oxygen generation (Arapoglou et al., 2003). We found that the lost energy in the form of heat was higher in the presence of lower concentrations of monovalent electrolytes. The maximum increased temperature (19 °C, i.e. from 23 to 42 °C) was observed at 0.05 M NaCl electrolyte, with higher increment rates at the beginning stages of the electrolysis process. According to Table 1, at 0.20 M Na_2SO_4 the minimum energy was utilized for the reduction of 1 kg of COD, and hence, the highest anode efficiency (AF) was attained. In this case, poor values were obtained for NaCl solutions, because of low COD removal efficiencies in the sodium chloride electrolyte.

3.5. Identification of organic intermediates

To identify organic by-products along electrochemical oxidation of CMP, 450 mL working solution containing 200 mg L⁻¹ CMP and 0.10 M Na_2SO_4 at pH 7 was electrolyzed at 33.33 mA cm⁻² for 300 min. The products of partial oxidation were

extracted by liquid-liquid extraction and analyzed by GC-MS. Under these conditions, 69% of the initial organic matter was completely oxidized to mineral products, i.e. CO₂ and water. This was mainly because of electrogenerated $\cdot OH$ radicals attacking organic structures, which led to the formation of various intermediates. $\cdot OH$ radicals act nonspecifically in oxidation reactions with more affinity for heteroatom bonds, such as C-N, than for C-C or C-H bonds (Paola et al., 2006). GC-MS analysis indicated that the CMP molecule was detected at a retention time (t_r) of 24.283 min (Fig. 7). This peak disappeared after the electrolysis and instead, different peaks were eluted at shorter retention times. This confirmed that CMP was broken into compounds with lower molecular weights.

Three major intermediates detected were as follows: (a) tertbutyl alcohol (t_r = 5.597 min), (b) tertbutyl amine (t_r = 8.238 min), and (c) N-tert-butyl acetamide (t_r =12.660 min). These compounds were probably converted to carboxylic acids, mainly formic and oxalic, which are known to be the most refractory final by-products before being completely oxidized to CO₂ (Boye et al., 2006; Yoshihara and Muruganathan, 2009). Aliphatic carboxylic acids were reported in previous studies as intermediate products of pharmaceutical compounds such as β -blockers (Radjenovic et al., 2011), enrofloxacin (Guinea et al., 2010), sulfamethoxazole (Dirany et al., 2010), as well as 17 β -estradiol and Bisphenol A (Yoshihara and Muruganathan, 2009).

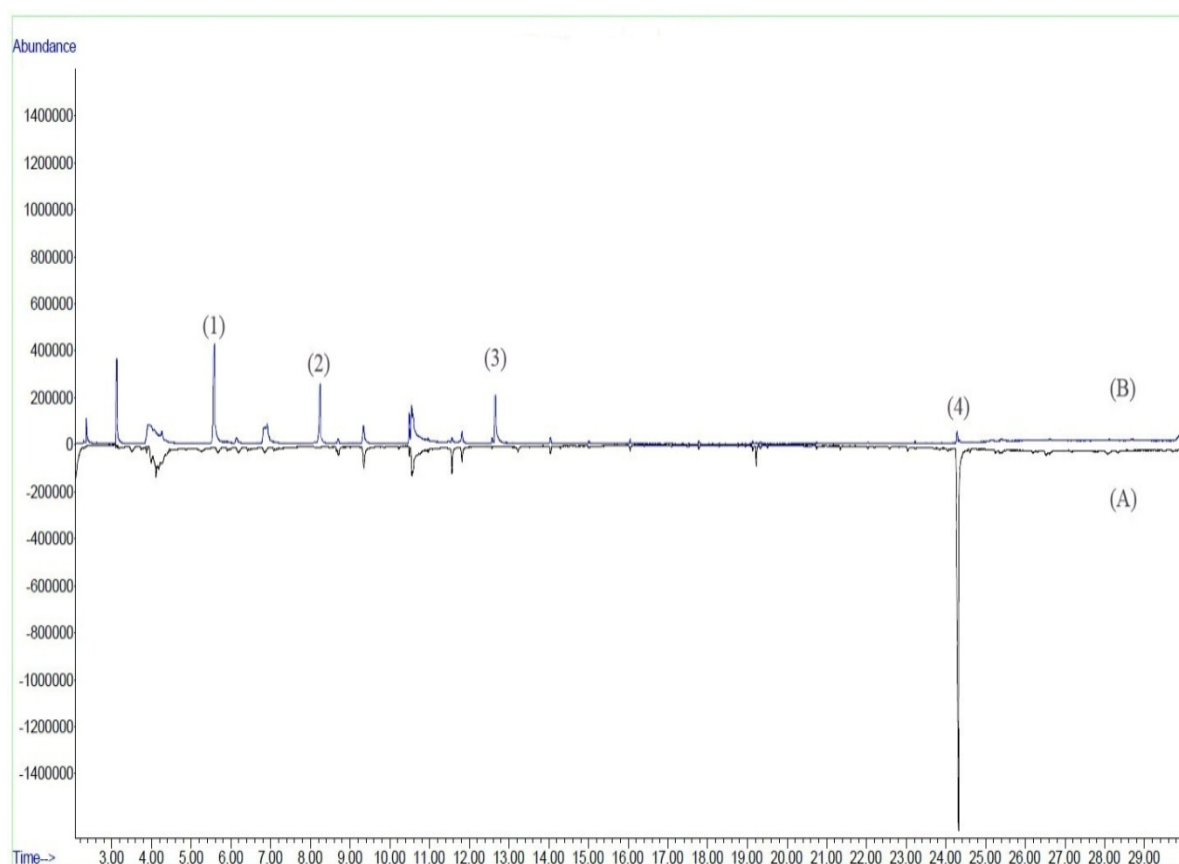


Fig. 7. GC-MS analysis of CMP solution (A) before and (B) after electrolysis (CMP concentration, 200 mg L⁻¹; pH, 7; current density, 33.33 mA cm⁻²; electrolyte, 0.10 M Na_2SO_4 , electrolysis time, 300 min)

4. Conclusions

The study showed that anodic oxidation of CMP under the experimental conditions was controlled by mass diffusion, obeying a pseudo-first-order kinetic law. The decay rate was found to increase with decreasing CMP concentrations, increasing current densities, and increasing initial pH.

The COD removal increased with decreasing initial concentrations; however, it was pH independent. Tert-butyl compounds were the major organic intermediates of CMP degradation. Based on the results obtained, it can be concluded that electrochemical oxidation is a feasible method for pre-and/or post-treatment of wastewaters containing biologically refractory organic pollutants such as pharmaceutical compounds.

Acknowledgements

The authors would like to thank the Vice Chancellor for Research and Technology, Iran University of Medical Sciences, Tehran, Iran, for funding the study.

References

- Abdel-Hamid R., Rabia M.K., Newair E.F., (2016), Electrochemical behaviour of antioxidants: Part 2. Electrochemical oxidation mechanism of quercetin at glassy carbon electrode modified with multi-walls carbon nanotubes, *Arabian Journal of Chemistry*, **9**, 350-356.
- Ahmed Basha C., Soloman P.A., Velan M., Miranda L.R., Balasubramanian N., Siva R., (2010), Electrochemical degradation of specialty chemical industry effluent, *Journal of Hazardous Materials*, **176**, 154-164.
- Arapoglou D., Vlyssides A., Israilides C., Zorpas A., Karlis P., (2003), Detoxification of methyl-parathion pesticide in aqueous solutions by electrochemical oxidation, *Journal of Hazardous Materials*, **98**, 191-199.
- Asazawa K., Yamada K., Tanaka H., Taniguchi M., Oguro K., (2009), Electrochemical oxidation of hydrazine and its derivatives on the surface of metal electrodes in alkaline media, *Journal of Power Sources*, **191**, 362-365.
- Asgari G., Rahmani A.R., Barjasteh Askari F., Godini K., (2012), Catalytic ozonation of phenol using copper coated pumice and zeolite as catalysts, *Journal of Research in Health Sciences*, **12**, 93-97.
- Bagastyo A.Y., Batstone D.J., Kristiana I., Gernjak W., Joll C., Radjenovic J., (2012), Electrochemical oxidation of reverse osmosis concentrate on boron-doped diamond anodes at circumneutral and acidic pH, *Water Research*, **46**, 6104-6112.
- Belhadj Tahar N., Abdelhédi R., Savall A., (2009), Electrochemical polymerisation of phenol in aqueous solution on a Ta/PbO₂ anode, *Journal of Applied Electrochemistry*, **39**, 663-669.
- Belhadj Tahar N., Savall A., (2009), Electropolymerization of phenol on a vitreous carbon electrode in alkaline aqueous solution at different temperatures, *Electrochimica Acta*, **55**, 465-469.
- Bensalah N., Alfaro M.A., Martínez-Huitle C.A., (2009), Electrochemical treatment of synthetic wastewaters containing Alphazurine A dye, *Chemical Engineering Journal*, **149**, 348-352.
- Boye B., Brillas E., Marselli B., Michaud P.A., Comminellis C., Farnia G., Sandonà G., (2006), Electrochemical incineration of chloromethylphenoxy herbicides in acid medium by anodic oxidation with boron-doped diamond electrode, *Electrochimica Acta*, **51**, 2872-2880.
- Brillas E., Sirés I., Arias C., Cabot P.L., Centellas F., Rodríguez R.M., Garrido J.A., (2005), Mineralization of paracetamol in aqueous medium by anodic oxidation with a boron-doped diamond electrode, *Chemosphere*, **58**, 399-406.
- Chatzisyseon E., Dimou A., Mantzavinos D., Katsaounis A., (2009), Electrochemical oxidation of model compounds and olive mill wastewater over DSA electrodes: 1. The case of Ti/IrO₂ anode, *Journal of Hazardous Materials*, **167**, 268-274.
- Chen J.L., Chiou G.C., Wu C.C., (2010), Electrochemical oxidation of 4-chlorophenol with granular graphite electrodes, *Desalination*, **264**, 92-96.
- Chen X., Chen G., (2005), Stable Ti/RuO₂-Sb₂O₅-SnO₂ electrodes for O₂ evolution, *Electrochimica Acta*, **50**, 4155-4159.
- Chen X., Gao F., Chen G., (2005), Comparison of Ti/BDD and Ti/SnO₂-Sb₂O₅ electrodes for pollutant oxidation, *Journal of Applied Electrochemistry*, **35**, 185-191.
- Chen X., Yao P., Wang D., Wu X., (2009), Antimony and cerium co-doped tin oxide electrodes for pollutant degradation, *Chemical Engineering Journal*, **147**, 412-415.
- Costa C.R., Montilla F., Morallón E., Olivi P., (2009), Electrochemical oxidation of acid black 210 dye on the boron-doped diamond electrode in the presence of phosphate ions: Effect of current density, pH, and chloride ions, *Electrochimica Acta*, **54**, 7048-7055.
- Costa C.R., Montilla F., Morallón E., Olivi P., (2010), Electrochemical oxidation of synthetic tannery wastewater in chloride-free aqueous media, *Journal of Hazardous Materials*, **180**, 429-435.
- Dalvand A., Gholami M., Joneidi A., Mahmoodi N.M., (2011), Dye removal, energy consumption and operating cost of electrocoagulation of textile wastewater as a clean process, *Clean-Soil, Air, Water*, **39**, 665-672.
- Davoudi M., Gholami M., Naseri S., Mahvi A.H., Farzadkia M., Esrafil A., Alidadi H., (2014), Application of electrochemical reactor divided by cellulosic membrane for optimized simultaneous removal of phenols, chromium, and ammonia from tannery effluents, *Toxicological & Environmental Chemistry*, **96**, 1310-1332.
- Del Rio A.I., Molina J., Bonastre J., Cases F., (2009), Study of the electrochemical oxidation and reduction of CI Reactive Orange 4 in sodium sulphate alkaline solutions, *Journal of Hazardous Materials*, **172**, 187-195.
- Dirany A., Sirés I., Oturan N., Oturan M.A., (2010), Electrochemical abatement of the antibiotic sulfamethoxazole from water, *Chemosphere*, **81**, 594-602.
- Eaton A., Clesceri L., Greenberg A., (2005), *Standard Methods for Examination of Water and Wastewater*, Washington, DC.
- Farzadkia M., Rahmani K., Gholami M., Esrafil A., Rahmani A., Rahmani H., (2014), Investigation of photocatalytic degradation of clindamycin antibiotic by using nano-ZnO catalysts, *Korean Journal of Chemical Engineering*, **31**, 2014-2019.

- Feng Y.J., Li X.Y., (2003), Electro-catalytic oxidation of phenol on several metal-oxide electrodes in aqueous solution, *Water Research*, **37**, 2399-2407.
- Gao J., Zhao G., Shi W., Li D., (2009), Microwave activated electrochemical degradation of 2, 4-dichlorophenoxyacetic acid at boron-doped diamond electrode, *Chemosphere*, **75**, 519-525.
- Gholami M., Rahmani K., Rahmani A., Rahmani H., Esrafil A., (2016), Oxidative degradation of clindamycin in aqueous solution using nanoscale zero-valent iron/H₂O₂/US, *Desalination and Water Treatment*, **57**, 13878-13886.
- Goyal R.N., Gupta V.K., Chatterjee S., (2008), Electrochemical oxidation of 2', 3'-dideoxyadenosine at pyrolytic graphite electrode, *Electrochimica Acta*, **53**, 5354-5360.
- Grčić I., Koprivanac N., Andričević R., (2017), Reliability study of laboratory scale water treatment by advanced oxidation processes, *Environmental Engineering and Management Journal*, **16**, 1-13.
- Guinea E., Garrido J.A., Rodríguez R.M., Cabot P.L., Arias C., Centellas F., Brillas E., (2010), Degradation of the fluoroquinolone enrofloxacin by electrochemical advanced oxidation processes based on hydrogen peroxide electrogeneration, *Electrochimica Acta*, **55**, 2101-2115.
- He Z., Huang C., Wang Q., Jiang Z., Chen J., Song S., (2011), Preparation of a Praseodymium Modified Ti/SnO₂-Sb/PbO₂ Electrode and its Application in the Anodic Degradation of the Azo Dye Acid Black 194, *International Journal of Electrochemical Science*, **6**, 4341-4354.
- Hmani E., Chaabane Elaoud S., Samet Y., Abdelhédi R., (2009), Electrochemical degradation of waters containing O-Toluidine on PbO₂ and BDD anodes, *Journal of Hazardous Materials*, **170**, 928-933.
- Jeong J., Lee J., (2012), Electrochemical oxidation of industrial wastewater with the tube type electrolysis module system, *Separation and Purification Technology*, **84**, 35-40.
- Kipp J.E., Smith W.J., Myrdal P.B., (1991), Determination of phosphate functional group acid dissociation constants of clindamycin 2-phosphate using 31 P Fourier transform NMR spectrometry, *International Journal of Pharmaceutics*, **74**, 215-220.
- Kong Y., Wang Z., Wang Y., Yuan J., Chen Z., (2011), Degradation of methyl orange in artificial wastewater through electrochemical oxidation using exfoliated graphite electrode, *New Carbon Materials*, **26**, 459-464.
- Li H., Zhu X., Jiang Y., Ni J., (2010), Comparative electrochemical degradation of phthalic acid esters using boron-doped diamond and Pt anodes, *Chemosphere*, **80**, 845-851.
- Li S., van der Est A., Bunce N.J., (2009), Electrochemical oxidation of oxalate ion in the presence of fluoride ion, and radical analysis by ESR, *Electrochimica Acta*, **54**, 3589-3593.
- Li X., Cui Y., Feng Y., Xie Z., Gu J.D., (2005), Reaction pathways and mechanisms of the electrochemical degradation of phenol on different electrodes, *Water Research*, **39**, 1972-1981.
- Liu Y., Liu H., Ma J., Li J., (2012), Preparation and electrochemical properties of Ce-Ru-SnO₂ ternary oxide anode and electrochemical oxidation of nitrophenols, *Journal of Hazardous Materials*, **213-214**, 222-229.
- Lutic D., Coromelci C.-G., Juzsakova T., Cretescu I., (2017), New mesoporous titanium oxide-based photoactive materials for the removal of dyes from wastewaters, *Environmental Engineering and Management Journal*, **16**, 801-807.
- Martínez-Huitile C.A., Ferro S., Reyna S., Cerro-López M., De Battisti A., Quiroz M.A., (2008), Electrochemical oxidation of oxalic acid in the presence of halides at boron doped diamond electrode, *Journal of the Brazilian Chemical Society*, **19**, 150-156.
- Martinez J.L., (2009), Environmental pollution by antibiotics and by antibiotic resistance determinants, *Environmental Pollution*, **157**, 2893-2902.
- Michaud P.A., Panizza M., Ouattara L., Diaco T., Foti G., Comninellis C., (2003), Electrochemical oxidation of water on synthetic boron-doped diamond thin film anodes, *Journal of Applied Electrochemistry*, **33**, 151-154.
- Montilla F., Morallón E., De Battisti A., Vázquez J.L., (2004), Preparation and characterization of antimony-doped tin dioxide electrodes. Part I. Electrochemical characterization, *The Journal of Physical Chemistry B*, **108**, 5036-5043.
- Murugananthan M., Latha S.S., Bhaskar Raju G., Yoshihara S., (2010), Anodic oxidation of ketoprofen - An anti-inflammatory drug using boron doped diamond and platinum electrodes, *Journal of Hazardous Materials*, **180**, 753-758.
- Murugananthan M., Yoshihara S., Rakuma T., Uehara N., Shirakashi T., (2007), Electrochemical degradation of 17 β -estradiol (E2) at boron-doped diamond (Si/BDD) thin film electrode, *Electrochimica Acta*, **52**, 3242-3249.
- Murugananthan M., Yoshihara S., Rakuma T., Shirakashi T., (2008), Mineralization of bisphenol A (BPA) by anodic oxidation with boron-doped diamond (BDD) electrode, *Journal of Hazardous Materials*, **154**, 213-220.
- Najafpoor A.A., Davoudi M., Salmani E.R., (2017), Decolorization of synthetic textile wastewater using electrochemical cell divided by cellulosic separator, *Journal of Environmental Health Science and Engineering*, **15**, DOI 10.1186/s40201-017-0273-3.
- Najafpoor A.A., Davoudi M., Salmani E.R., (2017), Optimization of copper removal from aqueous solutions in a continuous electrochemical cell divided by cellulosic separator, *Water Science and Technology*, **75**, 1233-1242.
- Palma-Goyes R.E., Guzmán-Duque F.L., Peñuela G., González I., Nava J.L., Torres-Palma R.A., (2010), Electrochemical degradation of crystal violet with BDD electrodes: Effect of electrochemical parameters and identification of organic by-products, *Chemosphere*, **81**, 26-32.
- Panizza M., Cerisola G., (2005), Application of diamond electrodes to electrochemical processes, *Electrochimica Acta*, **51**, 191-199.
- Panizza M., Michaud P., Cerisola G., Comninellis C., (2001), Anodic oxidation of 2-naphthol at boron-doped diamond electrodes, *Journal of Electroanalytical Chemistry*, **507**, 206-214.
- Paola A.D., Addamo M., Augugliaro V., Garcia-Lopez E., Loddò V., Marc G., Palmisano L., (2006), Photodegradation of lincomycin in aqueous solution, *International Journal of Photoenergy*, **8**, 1-6.
- Polcaro A.M., Vacca A., Mascia M., Palmas S., (2005), Oxidation at boron doped diamond electrodes: an effective method to mineralise triazines, *Electrochimica Acta*, **50**, 1841-1847.
- Radjenovic J., Bagastyo A., Rozendal R.A., Mu Y., Keller J., Rabaey K., (2011), Electrochemical oxidation of

- trace organic contaminants in reverse osmosis concentrate using RuO₂/IrO₂-coated titanium anodes, *Water Research*, **45**, 1579-1586.
- Radjenovic J., Escher B.I., Rabaey K., (2011), Electrochemical degradation of the β -blocker metoprolol by Ti/Ru_{0.7}Ir_{0.3}O₂ and Ti/SnO₂-Sb electrodes, *Water Research*, **45**, 3205-3214.
- Raghu S., Lee C.W., Chellammal S., Palanichamy S., Basha C.A., (2009), Evaluation of electrochemical oxidation techniques for degradation of dye effluents - A comparative approach, *Journal of Hazardous Materials*, **171**, 748-754.
- Rajkumar D., Guk Kim J., Palanivelu K., (2005), Indirect electrochemical oxidation of phenol in the presence of chloride for wastewater treatment, *Chemical Engineering & Technology*, **28**, 98-105.
- Ravikumar K., Sridhar B., (2010), Clindamycin hydrochloride monohydrate and its ethanol solvate, *Acta Crystallographica Section C: Crystal Structure Communications*, **66**, o97-o100.
- Samet Y., Agengui L., Abdelhédi R., (2010), Electrochemical degradation of chlorpyrifos pesticide in aqueous solutions by anodic oxidation at boron-doped diamond electrodes, *Chemical Engineering Journal*, **161**, 167-172.
- Samet Y., Elaoud S.C., Ammar S., Abdelhedi R., (2006), Electrochemical degradation of 4-chloroguaiacol for wastewater treatment using PbO₂ anodes, *Journal of Hazardous Materials*, **138**, 614-619.
- Serrano K., Michaud P.A., Comminellis C., Savall A., (2002), Electrochemical preparation of peroxodisulfuric acid using boron doped diamond thin film electrodes, *Electrochimica Acta*, **48**, 431-436.
- Sirés I., Brillas E., (2012), Remediation of water pollution caused by pharmaceutical residues based on electrochemical separation and degradation technologies: A review, *Environment International*, **40**, 212-229.
- Sirés I., Brillas E., Cerisola G., Panizza M., (2008), Comparative depollution of mecoprop aqueous solutions by electrochemical incineration using BDD and PbO₂ as high oxidation power anodes, *Journal of Electroanalytical Chemistry*, **613**, 151-159.
- Skoumal M., Arias C., Cabot P.L., Centellas F., Garrido J.A., Rodríguez R.M., Brillas E., (2008), Mineralization of the biocide chloroxyleneol by electrochemical advanced oxidation processes, *Chemosphere*, **71**, 1718-1729.
- Song S., Fan J., He Z., Zhan L., Liu Z., Chen J., Xu X., (2010), Electrochemical degradation of azo dye CI Reactive Red 195 by anodic oxidation on Ti/SnO₂-Sb/PbO₂ electrodes, *Electrochimica Acta*, **55**, 3606-3613.
- Song S., Zhan L., He Z., Lin L., Tu J., Zhang Z., Chen J., Xu L., (2010), Mechanism of the anodic oxidation of 4-chloro-3-methyl phenol in aqueous solution using Ti/SnO₂-Sb/PbO₂ electrodes, *Journal of Hazardous Materials*, **175**, 614-621.
- Tavares M.G., da Silva L.V.A., Sales Solano A.M., Tonholo J., Martínez-Huitle C.A., Zanta C.L.P.S., (2012), Electrochemical oxidation of Methyl Red using Ti/Ru_{0.3}Ti_{0.7}O₂ and Ti/Pt anodes, *Chemical Engineering Journal*, **204-206**, 141-150.
- Turro E., Giannis A., Cossu R., Gidaracos E., Mantzavinos D., Katsaounis A., (2011), Electrochemical oxidation of stabilized landfill leachate on DSA electrodes, *Journal of Hazardous Materials*, **190**, 460-465.
- Verdier L., Bertho G., Gharbi-Benarous J., Girault J.P., (2000), Lincomycin and clindamycin conformations. A fragment shared by macrolides, ketolides and lincosamides determined from TRNOE ribosome-bound conformations, *Bioorganic & Medicinal Chemistry*, **8**, 1225-1243.
- Vicent F., Morallon E., Quijada C., Vazquez J.L., Aldaz A., Cases F., (1998), Characterization and stability of doped SnO₂ anodes, *Journal of Applied Electrochemistry*, **28**, 607-612.
- Wang Y.H., Chan K.Y., Li X.Y., So S.K., (2006), Electrochemical degradation of 4-chlorophenol at nickel-antimony doped tin oxide electrode, *Chemosphere*, **65**, 1087-1093.
- Yoshihara S., Muruganathan M., (2009), Decomposition of various endocrine-disrupting chemicals at boron-doped diamond electrode, *Electrochimica Acta*, **54**, 2031-2038.
- Zaviska F., Drogui P., Blais J.F., Mercier G., Lafrance P., (2011), Experimental design methodology applied to electrochemical oxidation of the herbicide atrazine using Ti/IrO₂ and Ti/SnO₂ circular anode electrodes, *Journal of Hazardous Materials*, **185**, 1499-1507.
- Zhang Y., Xiong X., Han Y., Zhang X., Shen F., Deng S., Xiao H., Yang X., Yang G., Peng H., (2012), Photoelectrocatalytic degradation of recalcitrant organic pollutants using TiO₂ film electrodes: An overview, *Chemosphere*, **88**, 145-155.
- Zhao G., Shen S., Li M., Wu M., Cao T., Li D., (2008), The mechanism and kinetics of ultrasound-enhanced electrochemical oxidation of phenol on boron-doped diamond and Pt electrodes, *Chemosphere*, **73**, 1407-1413.
- Zhu X., Ni J., Wei J., Xing X., Li H., Jiang Y., (2010), Scale-up of BDD anode system for electrochemical oxidation of phenol simulated wastewater in continuous mode, *Journal of Hazardous Materials*, **184**, 493-498.